





Laser fluorescence spectroscopy in predicting the formation of a keloid scar: preliminary results and the role of lipopigments

ANDREEVA VIKTORIYA, RAZNITSYNA IRINA, *  GERZHIK ANASTASIIA,  GLAZKOV ALEXEY, MAKMATOV-RYS MIKHAIL, BIRLOVA ELEONORA, CHURSINOVA YULIYA, BOBROV MAKSIM, ROGATKIN DMITRY, SIPKIN ALEKSANDR, AND KULIKOV DMITRY

Moscow Regional Research and Clinical Institute, 61/2 Shchepkina str., Moscow, 129110, Russia

*RaznitsynaI@yandex.ru

Abstract: Keloid scars, in contrast to other scar types, significantly reduce the patient's quality of life. To develop a nondestructive optical diagnostic technique predicting the keloid scars formation *in vivo*, laser-induced fluorescence spectroscopy (LFS) was used to study the autofluorescence in skin of patients with various types of head and neck cicatricial deformities. The unexpected results were obtained for the endogenous fluorescence of lipofuscin. Significantly reduced autofluorescence of lipofuscin was registered both in the intact and in the keloid scar tissues in comparison with the intact and scar tissues in patients with hypertrophic and normotrophic scars. Sensitivity and specificity achieved by LFS in keloid diagnosis are 81.8% and 93.9% respectively. It could take place due to the changes in the reductive-oxidative balance in cells, as well as due to the proteolysis processes violation. Therefore, we suppose that the evaluation of the lipofuscin autofluorescence in skin before any surgical intervention could predict the probability of the subsequent keloid scars formation.

© 2020 Optical Society of America under the terms of the [OSA Open Access Publishing Agreement](#)

1. Introduction

Imaging or spectroscopy techniques used *in vivo* and based on autofluorescence in medical applications, consist in recording emitted light by endogenous fluorophores after the excitation of biological tissue with monochromatic light. The laser fluorescence spectroscopy (LFS) is based on recording of fluorescence spectra. As for the practical medicine, the LFS *in vivo* is applied mainly for cancer monitoring at the photodynamic therapy as well as for the intraoperative navigation held while defining borders of malignant neoplasms [1,2].

The fluorescence spectrum registered on the surface of biological tissues is determined by their biochemical composition. The fluorescence intensity increases with the proliferating number of the fluorescence emitting atoms and molecules, that is, in accordance with the changes of local concentration of the endogenous fluorophores in the area under examination. Therefore, it is possible to make indirect assumptions concerning their content in the biological tissue from the detected fluorescence intensity at the certain wavelengths corresponding to the radiation range of the individual structural components. Respectively, collagen, lipofuscin and porphyrin fluorescence are observed in the near UV, green and red spectral ranges [3]. Thus, the fluorescence spectra and their quantitative analysis could provide the information for the evaluation of the biological tissues condition. Whereas the method is sensitive to the minor changes in the biochemical tissue composition, it makes it possible to diagnose a number of pathologies at early stages [4–8].

The diagnostic potential of LFS method can be much wider than it is realized nowadays. For example, our recent studies in animals have shown that the tissue porphyrin content index in biological tissues calculated by means of the registered fluorescence spectra reflects the dynamics

of the local acute inflammatory process [9]. In combination with the optical tissue oximetry, LFS allows us to define quantitatively the stage of the fibrosis development and the prevailing pathological process (inflammation/ hypoxia/fibrosis) [10].

The study of the skin fibrosis was continued in the light of the research on fluorescent properties of the various scar types.

The following types of scars: normotrophic, hypertrophic, atrophic and keloid, which are varied by etiology, pathogenesis, structure and clinical manifestations are distinguished. The keloid and hypertrophic scars, in contrast with normotrophic and atrophic scars, are characterized by the formation of a dense, red scar cushion with irregular shape, and may be accompanied by itching, burning and local hyperthermia [11]. Also, they have the aesthetically unattractive appearance, therefore they significantly reduce the patient's quality of life. Most therapeutic approaches remain clinically unsatisfactory, in particular, because of poor understanding of the complex scarring mechanisms.

Clinical differentiation between hypertrophic scars and keloids is problematic especially at early stages. Classic guides consider keloids and hypertrophic scars as different scar types [11]. Clinicians define hypertrophic scars as tissues that do not extend beyond the primary wound, and keloids as scars that spread to surrounding healthy skin. Pathologists make a histological difference between keloids and hypertrophic scars based on thick, hyalinized collagen bundles in keloids. Such collagen is present in keloids, but can also be found in hypertrophic scars. There are many cases when the scar carries histological features of both hypertrophic and keloid scars. Some researchers suggest that hypertrophic and keloid scars can be considered as successive stages of the same fibroproliferative skin disease, with varying degrees of inflammation linked to a genetic predisposition [12]. In our paper, we adhere to the classical approach to the differentiation of scars based on the growth patterns and histological analysis.

It is customary to distinguish three phases of wound repair follow a specific time sequence: inflammation (I), proliferation (II) and remodeling (III) [13]. During the first two phases, an immune infiltrate is formed, which consists macrophages, mast cells, polymorphonuclear leukocytes, and the proliferation and accumulation of fibroblasts also begins, while deposition of dense collagen is not yet observed. It is important to mention that at these early stages of wound healing, pressure therapy and anti-inflammatory therapy are most effective and appropriate, which can reduce the size of the future scar and improve the prognosis for the patient. At the remodeling stage, the number of immune cells decreases and collagen fibers predominate, which are resistant to any type of therapy.

Frequently the diagnostics of keloid scars is carried out at the last phase and based on the clinical picture and the patient's medical history. The formed keloid scar treatment is often ineffective and, as a rule, involves surgical intervention. Although any damaging effect only provokes the pathology and leads to its recrudescence. To reduce the probability of the recurrence, modern medicine proposes immunomodulatory drugs [14], intralesional chemotherapy [15], the use of radiation therapy (excision followed by adjuvant irradiation) [16], which implies the patient radiation load. Therefore, extremely important for high-risk patients to avoid injuries, burns, unnecessary surgeries, injections, etc., and if surgical treatment is necessary, it is crucial to take preventive measures and to start the therapy at the earliest possible stage, for example, with the use of intralesional steroids, silicone-based products (i.e. gels, sheets and tapes) etc. [17,18].

As mentioned above, distinguishing the early-stage keloid from the hypertrophic scar histopathologically is very difficult [19]; therefore the use of labour-intensive and resource-consuming immunohistochemical methods is necessary. The practice shows that the clinical signs also do not always give a complete picture of the processes occurring in the scar tissue. Hence, today the search for non-invasive and objective methods of the keloid scar differentiation is an important task.

Among the non-invasive methods that can be used to diagnose scars the following may be pointed out: ultrasonography, laser Doppler flowmetry, narrow-band spectrophotometric color analysis, and other methods [20]. Multiphoton microscopy based on two-photon excited fluorescence (TPEF) and second harmonic generation (SHG) makes it possible to visualize the differences in the structure of the hypertrophic scar collagen and of the normal tissue collagen in patients of different ages [21].

The study performed by Hsu et al [22] describes the possibility of classifying the keloid scar severity and its therapeutic response based on the determination of the collagen and water content and the oxygen saturation by the method of diffuse scattering spectroscopy (DSR). Thus, the changes in the optical and fluorescence properties of the tissues during the process of wound repair are left in no doubt. There appears a question whether there are these differences between the types of cicatricial deformities.

The first results of the applicability of the LFS for the prediction of the keloid scar development are presented.

2. Materials and methods

Due to the fact that the main patients asking for reconstructive plastic surgery are women, the study involved female patients with the cicatricial deformities of the head and neck areas. The age of the patients ranged from 19 to 82 (median age: 57). In total, 139 scars in 23 female patients were examined, 85 of them were defined as normotrophic, 32 - as hypertrophic and 22 - as keloid.

The fluorescence spectra of scar and intact tissue (contralateral or at a distance of 1-2 cm from the scar in accordance with its location) after their excitation by monochromatic radiation at wavelengths of $\lambda_e = 365$ nm, 535 nm and 635 nm were recorded. All the measurements were performed with the use of the multifunctional laser diagnostic system "LAKK-M" (SPE 'LAZMA' Ltd, Russia) in the 'Fluorescence' operation regime. To take into account the effect of a tissue blood supply on the fluorescence intensity, the relative blood volume V_b (total hemoglobin content) in the studied areas was measured with the use of the "Microcirculation" mode of the system which implements methods of the optical tissue oximetry [23,24].

In this device, the low-power radiation from the selected laser is delivered to the surface of the biological tissue through the lighting optical fibers of the fiber optic probe. During measurements, the optical probe's tip is put in a gentle contact with the examined tissues. Power of the laser radiation on a distal end of the optical fiber probe (on a surface of tissues) is around 5 mW. The secondary radiation is delivered to the spectrometer by the receiving fiber of the probe. Lighting and receiving optical fibers are made of silicon and display a core diameter of 0.1 mm. Lighting-receiving distance is 1 mm. The backscattered excitation wavelength (λ_e) intensity is 1000 times reduced (factor $\beta = 1000$) by a colored-glass rejection optical filter. A recording spectral range for all excitation wavelengths is 350-800 nm. Spectra are observed on a laptop. Examples of keloid scar treated during the study (Fig. 1(a)) and of the clinical configuration of illumination and autofluorescence spectral data acquisition (Fig. 1(b)) are shown in Fig. 1.

There are various ways of LFS data processing, among which the analysis of absolute and normalized to the intact region indices of fluorescence are distinguished [25]. The normalized indices allow evaluating changes in biological tissues relatively to the healthy area and defining the activity of pathological processes. In this study, we need to compare the fluorescent features of the biological tissues both for intact and for scar tissues. Therefore, for each measurement site we use three fluorophore content indices $\eta(\lambda_f)_{\lambda_e}$ calculated by the equation [24]:

$$\eta(\lambda_f)_{\lambda_e} = \frac{I_f(\lambda_f)}{I_f(\lambda_f) + I_e(\lambda_e)} \quad (1)$$

where $I_f(\lambda_f)$ is the fluorescence intensity at the fluorescence wavelength λ_f , $I_e(\lambda_e)$ is the recorded intensity of the initial laser radiation backscattered by the tissue at the fluorescence excitation

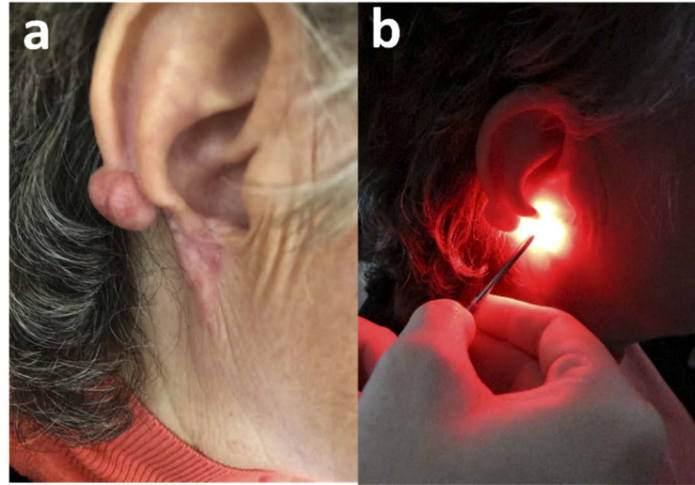


Fig. 1. a) Keloid scar on a woman aged 66 years, four years after surgery. Corticosteroids ongoing at the time of autofluorescence recording. b) Fiber probe tip is placed in a gentle contact with the keloid scar for autofluorescence spectra recording. Fluorescence excitation wavelength $\lambda_e=635$ nm.

wavelength (λ_e), reduced by the factor β ($\beta=1000$). Each index corresponds to the wavelength λ_e (365, 535 and 635 nm) and reflects the content of collagen, lipofuscin and porphyrin respectively. Thus, the collagen $\eta(455)_{365}$ (the effective fluorescence registration wavelength is $\lambda_f = 455$ nm [26]), lipofuscin $\eta(585)_{535}$ and porphyrin $\eta(670)_{635}$ - content indices were calculated.

Even though biological tissues contain many different fluorophores that fluoresce in the visible spectral range, we are able to evaluate the fluorescence of the above fluorophores, since their contribution to the total fluorescence spectrum at the indicated wavelengths is dominant. Besides, their spectra in the indicated waveband practically do not overlap [27].

Histological examination of scar tissue was performed according to the standard protocol with hematoxylin and eosin staining to verify the type of patients' cicatricial deformity.

The statistical analysis was performed with the use of IBM SPSS Statistics v25 software (IBM Corp., Armonk, New York, USA). There were held calculations of the arithmetic mean values and the standard deviations ($M \pm SD$) for the quantitative variables; as for the qualitative variables, the absolute frequencies were calculated. The comparison of the quantitative variables in the three groups was carried out using the Kruskal-Wallis test followed by the post-hoc analysis with the Dunn test adjusted for the multiple comparisons.

The differences were considered statistically significant at probability value $p < 0.05$. The prediction model for the scar type development was constructed using the logistic regression. The diagnostic capabilities of the constructed model and the selection of the cut-off point were evaluated using the ROC-analysis, during which the area under ROC curve (AUC) was calculated with a 95% confidence interval.

Independent Ethics Committee of Moscow Regional Research and Clinical Institute approved this study (protocol No. 4 on April 05, 2018). All patients provided informed consent before the study.

3. Results and discussion

According to the results of the histological analysis, all the examined scars were divided into groups in accordance to the revealed type of the cicatricial deformities. The typical histological images for the various scars and the healthy skin are presented in Fig. 2.

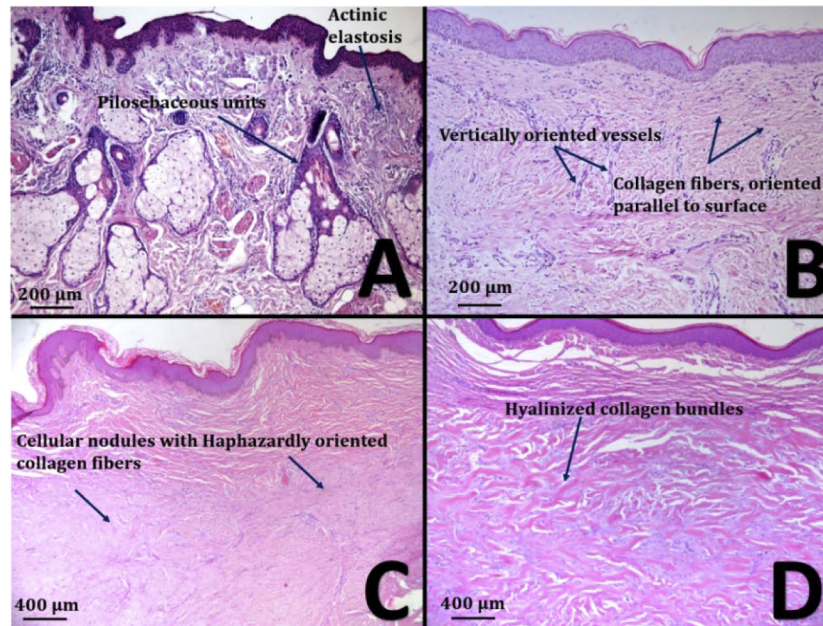


Fig. 2. The histological assessment of different cicatricial deformity types. Hematoxylin and eosin staining. A - normal skin: actinic elastosis manifestations in the upper dermis, pilosebaceous complexes; B - normotrophic scar: collagen fibers are oriented parallel to the skin surface. Vertically oriented vessels. Adnexal structures are absent; C - hypertrophic scar: nodular structures with the multidirectional collagen fibers, fibroblast proliferation; D - keloid scar: Wide hyalinized collagen ribbons.

The results of the LFS are presented in Table 1.

Table 1. The indices of the tissue fluorophores content $\eta(\lambda_f)_{\lambda_e}$ expressed in arbitrary units and a relative blood volume V_b (%) for normotrophic ($n = 85$), hypertrophic ($n = 32$), keloid scars ($n = 22$) and intact tissues.

	Index	Patients with normotrophic scars	Patients with hypertrophic scars	Patients with keloid scars	<i>p</i> -value (Kruskal-Wallis test)
Intact tissue	$\eta(455)_{365}$ a.u.	0.63 ± 0.12	0.60 ± 0.11	0.62 ± 0.06	0.462
	$\eta(585)_{535}$ a.u.	0.20 ± 0.07^c	0.20 ± 0.05^c	$0.12 \pm 0.06^{a, b}$	<0.001
	$\eta(670)_{635}$ a.u.	0.03 ± 0.01^b	0.04 ± 0.02^a	0.03 ± 0.01	0.038
	V_b , %	7.7 ± 2.7	8.3 ± 3.4	7.1 ± 2.7	
Scar	$\eta(455)_{365}$ a.u.	0.52 ± 0.13^c	0.50 ± 0.13^c	$0.27 \pm 0.13^{a, b}$	<0.001
	$\eta(585)_{535}$ a.u.	0.22 ± 0.12^c	0.26 ± 0.19^c	$0.05 \pm 0.04^{a, b}$	<0.001
	$\eta(670)_{635}$ a.u.	0.05 ± 0.05^c	0.07 ± 0.08^c	$0.03 \pm 0.01^{a, b}$	0.006
	V_b , %	12.5 ± 5.7	12.1 ± 7.1	10.0 ± 3.2	

The results of the post-hoc tests with the correction for multiple comparisons:

^astatistically significant difference with the normotrophic scar

^bstatistically significant differences with the hypertrophic scar

^cstatistically significant differences with the keloid scar

The analysis of the collagen, porphyrins, and lipofuscin fluorescence of the scar tissue showed statistically significant differences in the tissue indices of the lipofuscin content $\eta(585)_{535}$ and the

collagen content $\eta(455)_{365}$ between the keloid and the normal and hypertrophic scars (Table 1). However, in this case, it is not entirely correct to conclude that this dissimilarity is caused precisely by the deviations in the biochemical content of the scar tissue. The results of the LFS could be influenced by the age of the scar, its size and homogeneity. Moreover, the condition of the vascular bed in the scar after the surgery intervention, the presence of edema and hematomas also affects the light-absorbing and scattering properties of the biological tissue. Therefore, it is incorrect to determine the tissue indices of fluorophores content in the scar tissue as a differentiating criterion.

It occurred to be interesting that the statistically significant differences were identified in the tissue content index of lipofuscin in intact tissues in patients with keloid scars. An example of the recorded spectra is shown in Fig. 3. Taking into account the fact that the intact tissue with head/neck localization are not affected by the characteristics of the scar and its formation features, we made an assumption that the initial skin's state affects the formation of the scar, and this condition can be quantitatively described by LFS method.

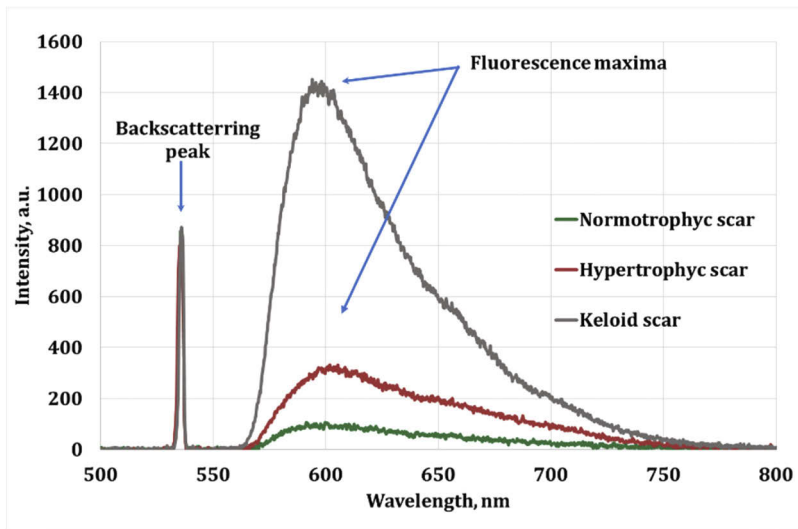


Fig. 3. An example of the healthy skin fluorescence spectra in patients with normotrophic (patient's age is 52 years, green curve), hypertrophic (61 years of age, red curve), keloid scar (28 years of age, grey curve) for excitation wavelength (λ_e) 535 nm.

It is known that changes in the optical properties of biological tissue due to changes in the blood supply may affect the interpretation of LFS data especially in the green spectral range [28]. However, no significant differences in the measured V_b between groups of patients with different types of scars were found (Tab.1). Therefore, the differences detected are related to fluorescent properties of the tissue. Consequently, it is possible to assess the probability of the keloid development in a particular patient by using LFS on the intact skin. Lipofuscin, also known as the aging pigment, is formed and accumulated as a result of the unsaturated fats oxidation or in the case of damage to the organelles' membranes [29], because its fluorescence in normal tissues is more acute in age-related patients.

The analysis performed in the IBM SPSS v25 program demonstrated that $\eta(585)_{535}$ is a statistically significant factor, which increases odds of keloid development. Since age was a confounding factor, it was also included in the logistic regression model for adjustment. It was determined that with the age adjustment AUC = 0.869 is higher than without it (AUC = 0.867).

Using the logistic regression method, a formula for assessing the keloid scar development probability depending on the patient's age a and $\eta(585)_{535}$ in the intact tissue was obtained:

$$P = \frac{1}{1 + e^{0.052 \cdot a + 20.991 \cdot \eta(585)_{535} - 3.928}} \quad (2)$$

The optimal value $P = 0.32$ was selected, at which the parameters of sensitivity and specificity were 81.8% and 93.9%, respectively. Thus, if the calculated probability value exceeds 0.32, it is possible to speak of the increased risk of the keloid scar formation for the patient.

According to the obtained formula (2) for the assessment of the keloid scar development probability, it could be identified that the young age and the low lipofuscin level are the risk factors for the keloid formation. According to the published data, keloid scars are indeed more common in young patients [30,31]. Figure 4 shows the correlation between the healthy skin average $\eta(585)_{535}$ on the age group of the patients. Similar data has been demonstrated in many studies, for example in [32] by Kakimoto. Represented formula (2) takes into consideration both patients' age and the individual variability of the skin condition linked to the various physiological and pathological processes, in particular, lifestyle, nutrition, hereditary background, etc.

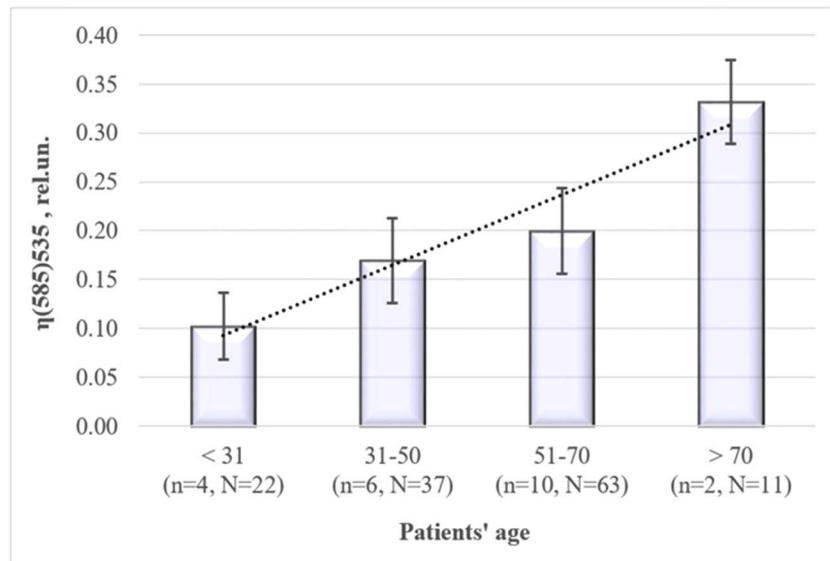


Fig. 4. The indices of the tissue lipofuscin healthy skin content $\eta(585)_{535}$ expressed in arbitrary units ($M \pm SD$) in different age groups. n – number of patients in each group; N – number of areas under investigation in each group.

The mechanisms of how the lipofuscin level in a patients' skin affect the type of the forming scar are not completely clear. There is a correlation between the lipofuscin production in the skin and the oxidative stress [33]. Reactive forms of oxygen contribute to the development of the skin fibrotic changes [34], as well. However, this does not lead to the direct link between the level of lipofuscin and the keloid formation risk due to the multifactorial nature of the processes mentioned above. The intracellular formation of lipofuscin is a complex network of reactions involving various cellular compartments and enzymes. At the same time, the high rate of lipofuscin accumulation decreases the cell lifespan [35]. It can be assumed, for example, that the lipofuscin accumulated in skin cells inhibits the formation of the keloid collagen, which is composed of disorganized I and III type collagen bundles and a relatively small number of fibroblasts [36–38]. Moreover, it was shown that the decrease in the proteolytic processes activity

in a cell is associated with the lipofuscin granules accumulation in it [39]. On the other hand, there is an evidence of the proteolytic enzymes activation in the case of the keloid scar formation: Akasaka et al. [40] showed that the increased expression of caspase-3 is observed in keloid scars, which leads to the induction of the apoptosis of the fibroblasts, which could play a role in the fibrosis formation.

Thus, the analysis of the laser fluorescence spectroscopy results of various types of cicatricial deformities as well as intact tissues suggests that the probability of the keloid scar formation could be determined by the endogenous fluorescence of the healthy patient's tissue. In terms of the specific design features of the experiment described above, we can conclude that the identification of the keloid development probability in a certain location could be predicted only by LFS performed in the contralateral healthy skin or in areas positioned at 1-2 cm distance from the scar margin. The analysis of the fluorescence diagnostic significance of other intact skin areas is the task of the following studies.

It is also worth noting that the proposed formula for the probability of the keloid scar formation (Eq. (2)) was obtained on the basis of the research results of the head and neck skin of patients with 2-3 Fitzpatrick phototypes. To develop a more universal formula which would take into account not only the fluorescence of lipofuscin in the skin and the patient's age, but also the melanin content, which affects the light absorption, as well as the scar localization, it is necessary to conduct a much larger study forming corresponding experimental groups.

4. Conclusion

The results of *in vivo* LFS in a patients' skin with various cicatricial deformities showed the possibility to predict a keloid scar formation examining the intact skin with sensitivity and specificity of 81.8% and 93.9% respectively. The results allow suggesting that the decreased endogenous lipofuscin fluorescence in the healthy patient's skin could serve as an optical marker for the increased probability of the keloid scar formation. However, further studies should be conducted, including histological and immunohistochemical ones, to confirm this preliminary conclusion.

The fact that the describe method involves the healthy skin analysis makes it more versatile. In the long run, LFS could form the basis for the method predicting the risk of the keloid scar formation even before the surgery intervention. Such a preventive diagnostic approach will help to take appropriate timely measures, basically including the full informing of the patient, avoiding skin injuries, the choice of the minimally traumatic surgical tactics, prolonged postoperative immobilization and the use of adhesive coatings with the silicone gel.

Furthermore, the low lipofuscin content in the healthy skin of patients prone to the keloid scar formation could make a fundamental contribution to the understanding of this pathology pathogenesis.

Funding

Russian Foundation for Basic Research (18-02-00564).

Disclosures

The authors declare no conflicts of interest.

References

1. S. Utsuki, H. Oka, S. Sato, S. Suzuki, S. Shimizu, S. Tanaka, and K. Fujii, "Possibility of using laser spectroscopy for the intraoperative detection of nonfluorescing brain tumors and the boundaries of brain tumor infiltrates," *J. Neurosurg.* **104**(4), 618–620 (2006).
2. G. M. Van Dam, G. Themelis, L. M. Crane, N. J. Harlaar, R. G. Pleijhuis, W. Kelder, A. Sarantopoulos, J. S. de Jong, H. J. G. Arts, A. G. J. van der Zee, J. Bart, P. S. Low, and V. Ntziachristos, "Intraoperative tumor-specific

- fluorescence imaging in ovarian cancer by folate receptor- α targeting: first in-human results,” *Nat. Med.* **17**(10), 1315–1319 (2011).
3. L. Bachmann, D. M. Zezell, A. D. C. Ribeiro, L. Gomes, and A. S. Ito, “Fluorescence spectroscopy of biological tissues—A review,” *Appl. Spectrosc. Rev.* **41**(6), 575–590 (2006).
 4. J. R. Lakowicz, *Principles of Fluorescence Spectroscopy* (Springer Science & Business Media, 2013).
 5. I. Georgakoudi, B. C. Jacobson, M. G. Müller, E. E. Sheets, K. Badizadegan, D. L. Carr-Locke, C. P. Crum, C. W. Boone, R. R. Dasari, J. Van Dam, and M. S. Feld, “NAD (P) H and collagen as in vivo quantitative fluorescent biomarkers of epithelial precancerous changes,” *Cancer Res.* **62**(3), 682–687 (2002).
 6. W. Rettig, B. Strehmel, S. Schrader, and H. Seifert, *Applied Fluorescence in Chemistry, Biology and Medicine* (Springer Science & Business Media, 2012).
 7. L. Marcu, J. A. Jo, Q. Fang, T. Papaioannou, T. Reil, J. H. Qiao, J. D. Baker, J. A. Freischlag, and M. C. Fishbein, “Detection of rupture-prone atherosclerotic plaques by time-resolved laser-induced fluorescence spectroscopy,” *Atherosclerosis* **204**(1), 156–164 (2009).
 8. A. F. Zandoná and D. T. Zero, “Diagnostic tools for early caries detection,” *J. Am. Dent. Assoc.* **137**(12), 1675–1684 (2006).
 9. E. N. Petritskaya, D. A. Kulikov, D. A. Rogatkin, I. A. Guseva, and P. A. Kulikova, “Use of fluorescence spectroscopy for diagnosis of hypoxia and inflammatory processes in tissue,” *J. Opt. Technol.* **82**(12), 810–814 (2015).
 10. Y. V. Chursinova, D. A. Kulikov, D. A. Rogatkin, I. A. Raznitsyna, D. V. Mosalskaya, M. A. Bobrov, E. N. Petritskaya, and A. V. Molochkov, “Laser fluorescent spectroscopy and optical tissue oximetry in diagnostics of skin fibrosis,” *Biomed. Photonics* **8**(1), 38–45 (2019).
 11. C. J. Chike-Obi, P. D. Cole, and A. E. Brissett, “Keloids: pathogenesis, clinical features, and management,” *Semin. Plast. Surg.* **23**(03), 178–184 (2009).
 12. C. Huang, S. Akaishi, H. Hyakusoku, and R. Ogawa, “Are keloid and hypertrophic scar different forms of the same disorder? A fibroproliferative skin disorder hypothesis based on keloid findings,” *Int. Wound J.* **11**(5), 517–522 (2014).
 13. G. G. Gauglitz, H. C. Korting, T. Pavicic, T. Ruzicka, and M. G. Jeschke, “Hypertrophic scarring and keloids: pathomechanisms and current and emerging treatment strategies,” *Mol. Med.* **17**(1-2), 113–125 (2011).
 14. A. Chuangsuwanich and S. Gunjittisomrarn, “The efficacy of 5% imiquimod cream in the prevention of recurrence of excised keloids,” *J. Med. Assoc. Thai.* **90**(7), 1363–1367 (2007).
 15. A. M. Wilson, “Eradication of keloids: surgical excision followed by a single injection of intralesional 5-fluorouracil and botulinum toxin,” *Can. J. Plast. Surg.* **21**(2), 87–91 (2013).
 16. M. C. E. van Leeuwen, S. C. Stokmans, A. E. J. Bulstra, O. W. M. Meijer, M. W. Heymans, J. C. F. Ket, M. J. P. F. Ritt, P. A. M. van Leeuwen, and F. B. Niessen, “Surgical excision with adjuvant irradiation for treatment of keloid scars: a systematic review,” *Plast. Reconstr. Surg. Glob. Open* **3**(7), e440 (2015).
 17. B. Berman, A. Maderal, and B. Raphael, “Keloids and hypertrophic scars: pathophysiology, classification, and treatment,” *Dermatol. Surg.* **43**(1), S3–S18 (2017).
 18. S. Al-Shaqsi and T. Al-Bulushi, “Cutaneous scar prevention and management: overview of current therapies,” *Sultan Qaboos Univ. Med. J.* **16**(1), e3–8 (2016).
 19. J. Y. Y. Lee, C. C. Yang, S. C. Chao, and T. W. Wong, “Histopathological differential diagnosis of keloid and hypertrophic scar,” *Am. J. Dermatopathol.* **26**(5), 379–384 (2004).
 20. D. M. Perry, D. A. McGrouther, and A. Bayat, “Current tools for noninvasive objective assessment of skin scars,” *Plast. Reconstr. Surg.* **126**(3), 912–923 (2010).
 21. G. Chen, J. Chen, S. Zhuo, S. Xiong, H. Zeng, X. Jiang, R. Chen, and S. Xie, “Nonlinear spectral imaging of human hypertrophic scar based on two-photon excited fluorescence and second-harmonic generation,” *Br. J. Dermatol.* **161**(1), 48–55 (2009).
 22. C. K. Hsu, S. Y. Tzeng, C. C. Yang, J. Y. Y. Lee, L. L. H. Huang, W. R. Chen, M. Hughes, Y. W. Chen, Y. K. Liao, and S. H. Tseng, “Non-invasive evaluation of therapeutic response in keloid scar using diffuse reflectance spectroscopy,” *Biomed. Opt. Express* **6**(2), 390–404 (2015).
 23. P. Rölfe, “In vivo near-infrared spectroscopy,” *Annu. Rev. Biomed. Eng.* **2**(1), 715–754 (2000).
 24. D. Rogatkin, V. Shumskiy, S. Tereshenko, and P. Polyakov, “Laser-based non-invasive spectrophotometry—an overview of possible medical applications,” *Photonics Lasers Med.* **2**(3), 225–240 (2013).
 25. I. Guseva, D. Rogatkin, P. Kulikova, and D. Kulikov, “In Vivo Experimental Detection of Inflammatory Process in Tissues by Fluorescence Spectroscopy,” *Proc. of the 9th Int. Joint Conference on Biomedical Engineering Systems and Technologies (BIOSTEC 2016), v.1: BIODEVICES*, 139–144 (2016).
 26. O. D. Smirnova, D. A. Rogatkin, and K. S. Litvinova, “Collagen as in vivo quantitative fluorescent biomarkers of abnormal tissue changes,” *J. Innovative Opt. Health Sci.* **05**(02), 1250010 (2012).
 27. N. Kollias, G. Zonios, and G. N. Stamatias, “Fluorescence spectroscopy of skin,” *Vib. Spectrosc.* **28**(1), 17–23 (2002).
 28. A. V. Dunaev, V. V. Dremmin, E. A. Zhrebtsov, I. E. Rafailov, K. S. Litvinova, S. G. Palmer, N. A. Stewart, S. G. Sokolovski, and E. U. Rafailov, “Individual variability analysis of fluorescence parameters measured in skin with different levels of nutritive blood flow,” *Med. Eng. Phys.* **37**(6), 574–583 (2015).
 29. A. Terman and U. T. Brunk, “Lipofuscin: mechanisms of formation and increase with age,” *APMIS* **106**(1-6), 265–276 (1998).

30. A. S. Halim, A. Emami, I. Salahshourifar, and T. P. Kannan, "Keloid scarring: understanding the genetic basis, advances, and prospects," *Arch. Plast. Surg.* **39**(3), 184 (2012).
31. A. G. Marneros, J. E. Norris, B. R. Olsen, and E. Reichenberger, "Clinical genetics of familial keloids," *Arch. Dermatol.* **137**(11), 1429–1434 (2001).
32. Y. Kakimoto, C. Okada, N. Kawabe, A. Sasaki, H. Tsukamoto, R. Nagao, and M. Osawa, "Myocardial lipofuscin accumulation in ageing and sudden cardiac death," *Sci. Rep.* **9**(1), 3304 (2019).
33. A. Moreno-Garcia, A. Kun, O. Calero, M. Medina, and M. Calero, "An overview of the role of lipofuscin in age-related neurodegeneration," *Front. Neurosci.* **12**, 464 (2018).
34. B. De Felice, C. Garbi, M. Santoriello, A. Santillo, and R. R. Wilson, "Differential apoptosis markers in human keloids and hypertrophic scars fibroblasts," *Mol. Cell. Biochem.* **327**(1-2), 191–201 (2009).
35. T. Jung, N. Bader, and T. Grune, "Lipofuscin: formation, distribution, and metabolic consequences," *Ann. N. Y. Acad. Sci.* **1119**(1), 97–111 (2007).
36. W. R. Blackburn and B. Cosman, "Histologic basis of keloid and hypertrophic scar differentiation," *Arch. Pathol.* **82**, 65–71 (1966).
37. I. F. K. Muir, "On the nature of keloid and hypertrophic scars," *Br. J. Plast. Surg.* **43**(1), 61–69 (1990).
38. D. D. Datubo-Braun, "Keloids. A review of the literature," *Br. J. Plast. Surg.* **43**(1), 70–77 (1990).
39. A. Höhn and T. Grune, "Lipofuscin: formation, effects and role of macroautophagy," *Redox Biol.* **1**(1), 140–144 (2013).
40. Y. Akasaka, Y. Ishikawa, I. Ono, K. Fujita, T. Masuda, N. Asuwa, K. Inuzuka, H. Kiguchi, and T. Ishii, "Enhanced expression of caspase-3 in hypertrophic scars and keloid: induction of caspase-3 and apoptosis in keloid fibroblasts in vitro," *Lab. Invest.* **80**(3), 345–357 (2000).